Optimal key design for shaft hub connections

Pedersen, Niels Leergaard

Published in:
Proceedings of the Institution of Mechanical Engineers, Part C: Journal of Mechanical Engineering Science

Link to article, DOI:
10.1177/09544062231174125

Publication date:
2024

Document Version
Peer reviewed version

Optimal key design for shaft hub connections

Niels Leergaard Pedersen
Dept. Civil and Mechanical Engineering, Solid Mechanics
Technical University of Denmark
Koppels Allé, Building 404, DK-2800 Kgs. Lyngby, Denmark
email: nlpe@dtu.dk

Abstract

Key connections in shaft hub assemblies are typically used due to the price of production but also the possibility for using it as an overload protection and safety device is important. The design of keyways and keys is specified in standards, different designs are available but typically the contact area is flat. The connection fatigue strength is improved if the stress concentration is reduced; important here is both the key shape and also the tolerances between key and keyway. The present designs described in standards are to some extend the result of previous possibilities for production. Today larger variations are possible without increasing the production price significantly. New designs with improved strength are presented and the design evaluation is done using both 2D and 3D finite element models including contact modelling. The design is primarily described by the super elliptical shape, i.e. the design parameterization is simple. Improvement in the stress level found is significant, a maximum reduction of 78% is found, indicating that the fatigue strength can be significantly increased.

Key words: Machine elements, key connection, torsion, stress concentration, FEA, 2D/3D.

1 Introduction

Key connections are one of the most simple shaft hub connections with design specifications available in standards see e.g. [1]. For other standard designs see general machine element books e.g. [2] or [3]. The points favouring a key connection is; low production cost, easy assembly/disassembly and the possibility for overload avoidance. The negative points are no axial fixation, low strength and uneven stress distribution in the contact. The typical solution to the problem of strength is to increase the key length or the number of keys used. With more keys there is a tolerance problem related to multiple keys engaging at the same time. In the limit a spline connection is used. For multiple keys or a spline connection the normal design rule is that 75% of the teeth are engaged (carry the load).

For all designs in standards it is such that the torsional moment can be transmitted equally well in reversed direction, i.e. the designs are symmetric. If a connection is to operate only in one direction we can make an unsymmetrical design that can improve the strength further.

The key connection strength can be evaluated in two ways depending on the load situation. For non-fatigue loading the strength is related to plastic bearing failure of the shaft and hub or the key shearing (ultimate strength), the latter is the case when the key connection is used

also as an overload safety device. Typically the stress is evaluated as a nominal stress when compared to material limits. The second case is the fatigue loading of the connection, in this case the maximum stress, i.e. the stress concentration, is controlling the strength, see [4] and [5]. In the present paper the focus is on the second case.

As discussed in [6] also with a reference to [7] little efforts have been used for standard key design modification. A proposal for simple modifications to improve the design is given in [7].

Evaluation of stress concentration can be performed experimentally but in relation to optimization the use of numerical methods and Finite Element Analysis (FEA) is the preferred method applied in the present paper. In a key connection we transfer the torsional moment through contact between shaft and key and key and hub, for a full stress evaluation we therefore need to include contact modelling. In a keyway design there is several positions in which the maximum stress might be found, e.g. in the keyway run-out where typically no contact with the key takes place. To improve the design we must reduce the maximum stress wherever it is found. In the present paper we do not investigate the stress state at the keyway run-out. Focus is on the peak stress in the contact regions. Generally the maximum stress is controlled by two factors; the geometric design and the size of load applied to the point. In a contact we also have singularities related to the run-out of contact, see e.g. [8], with the possibility for high stress. In [7] one simple modification suggested is to apply a circular hole close to the key ends for avoiding the high stress related to the contact run-out in the length direction of the key.

The loading of the shaft hub connection can in principle include torsion, bending, shear and tension, in the present paper we will assume pure torsion, see [9] in relation to other loads and load combinations.

The numerical modelling of the power transmission between shaft and hub involves contact modelling and the modelling of the load i.e. the transmitted torsional moment. In general it is not possible to model the transmission of torsional moment fully correct using a 2D contact model a 3D model is needed. As done in [6] we can model the pure torsion of a cross section using a 2D model. With a spline connection we have the possibility to apply symmetry to reduce the 3D modelling. This is however, not the case for a design with a single key and keyway. In [10] the results reported show that there is a difference in the maximum stress found if the torsion is performed with or without the key. The general findings is that the stress elevation is restricted to be a maximum of 24%. This indicate that a 2D modelling using pure torsion is sufficient. In the present paper it is shown that the difference in maximum stress found with or without the key and contact modelling is significant. Similarities in the stress variation found in full 3D contact modelling and a simplified 2D contact modelling show however that a simplified 2D contact model could be used for optimization purpose.

The standardized key and keyways are geometrically defined by straight lines and circular arches, which from a point of low stress are not optimal shapes. The optimization in the present paper is performed in order to reduce the stress concentration factor. The stress reduction is achieved through shape optimization where the shape to design is also where we have the contact. A simple analytical shape representation is applied using the super ellipse. This facilitates an optimization problem with a low number of design parameters (less than 13). With the small number of design parameters a simple parameter study to minimize the stress is possible. The simple shape representation and the number of design variables also enables a simple result communication making the designs in this regard more practical. With more design variables it will typically be possible to optimize the designs further. We know that the optimal shape is the one that result in a constant stress along the designed shape. If the optimization results in a constant stress the possible further improvement by a more involved parameterization can therefore be evaluated. As discussed in [11] we cannot use the FE nodes position as the design param-

eters. With stress minimization as the optimization objective it is also important that the FE stress level is converged which can be checked by a mesh refinement. With an analytical shape description that is not linked to the FE discretization this mesh refinement can be performed.

The paper is organized as follows. In Section 2 the super elliptic parameterization is presented mathematically, this design parameterization is used for the cross sectional key and keyway design. Section 3 describes the numerical modelling of torsion and the applied assumptions. The comparison of maximum stress found in the full 3D contact model and the simple 2D contact model is also discussed. The optimization using symmetric key design in presented in Section 4 where also a comparison to previous found optimized designs is made. In Section 5 the results assuming unsymmetrical design are presented. Conclusions are given in Section 6.

2 Super elliptic parameterization

One possibility for shape parameterization of the key is to use the super ellipse, see e.g. [12] and [13]. The initial shape has only three design parameters, principle axes A and B and super elliptical power η. The parametric form is

$$X = A\cos(t)^{(2/\eta)},\ t \in [0 : \frac{\pi}{2}] \tag{1}$$

$$Y = B\sin(t)^{(2/\eta)},\ t \in [0 : \frac{\pi}{2}] \tag{2}$$

Using this parameterization we can connect the two points (marked by a cross) in Figure 1a) and the shape will lie within the design domain indicated in grey. For $\eta > 2$ the curvature is zero at points A and B and for $\eta > 1$ the curve slope at points A and B follows the design domain boundaries.

In [14] the super ellipse is also used in a distorted form, with the parametric form

$$X = A\cos(t)^{(2/\eta)}(1 - \frac{B}{A}\tan(\beta)\sin(t)^{(2/\eta)}),\ t \in [0 : \frac{\pi}{2}] \tag{3}$$

$$Y = B\sin(t)^{(2/\eta)},\ t \in [0 : \frac{\pi}{2}] \tag{4}$$

With this parameterization the design domain is changed to the one shown in Figure 1b).

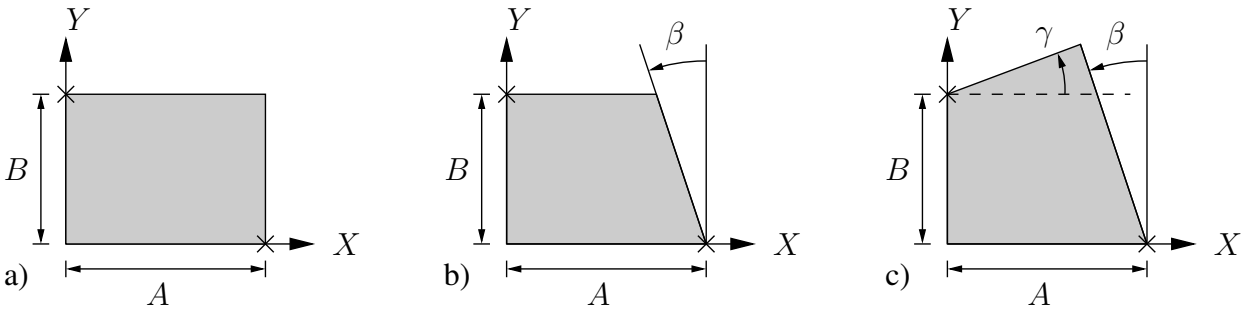

Figure 1: a) Design domain for super ellipse. b) Distorted super ellipse. c) Double distorted super ellipse.

A double distortion of the super ellipse as indicated by the design domain in Figure 1c) where two rotation angles are used is applied in [15]. The analytical form as given in [15] is

$$X = \left(A - B\sin(t)^{(2/\eta)}\tan(\beta)\right)\cos(t)^{(2/\eta)},\ t \in [0 : \frac{\pi}{2}] \tag{5}$$

$$Y = \left(B + \cos(t)^{(2/\eta)}(A - B\sin(t)^{(2/\eta)}\tan(\beta))\tan(\gamma)\right) \cdot \sin(t)^{(2/\eta)},\ t \in [0 : \frac{\pi}{2}] \tag{6}$$

With the parameterization in (5) and (6) we have a simple parameterization with two rotations but the shape might, depending on the sign of the angles γ and β violate the design domain.

With a slight modification (mapping) from Figure 1a) to 1c) we have the following analytical form instead

$$X = A\cos(t)^{(2/\eta)} + \cos(t)^{(2/\eta)}\sin(t)^{(2/\eta)} \cdot \left(\frac{A - B\tan(\beta)}{\tan(\gamma)\tan(\beta) + 1} - A\right),\ t \in [0 : \frac{\pi}{2}] \tag{7}$$

$$Y = B\sin(t)^{(2/\eta)} + \cos(t)^{(2/\eta)}\sin(t)^{(2/\eta)} \cdot \left(\frac{B + A\tan(\gamma)}{\tan(\gamma)\tan(\beta) + 1} - B\right),\ t \in [0 : \frac{\pi}{2}] \tag{8}$$

The parametric shape as described in (7) and (8) lies within the design domain 1c) and for $\eta > 2$ the curve curvature is zero at points A and B and for $\eta > 1$ the curve slope at points A and B follows the design domain boundaries.

In Figure 2 different curves are shown to illustrate this.

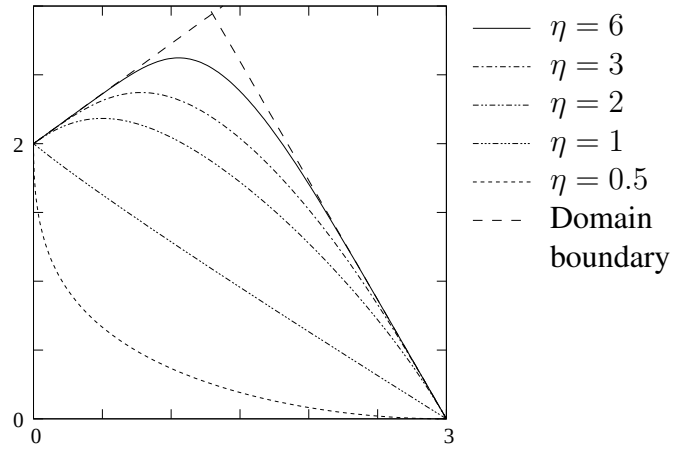

Figure 2: Examples of distorted super ellipse. The design domain is specified by $A = 3$, $B = 2$, $\beta = \pi/6$ and $\gamma = \pi/5$.

We now have the possibility to model each quarter of the key cross section in the axial direction by this distorted super ellipse. Applying this to the complete key cross-section and if we seek to have continuity also in slope and curvature we can make a model with 13 design parameters. An example of this is illustrated in Figure 3. If we seek a symmetric design this can easily be achieved with a reduced number of design parameters as the result. The 13 design parameters are shown in the figure. Please note that B_1 and B_2 are the principle axes for the distorted super ellipse in 1 quadrant and 3 quadrant respectively. The principle axes (Y direction) is then $b - B_2$ and $b - B_1$ for the distorted super ellipse in 2 quadrant and 4 quadrant respectively.

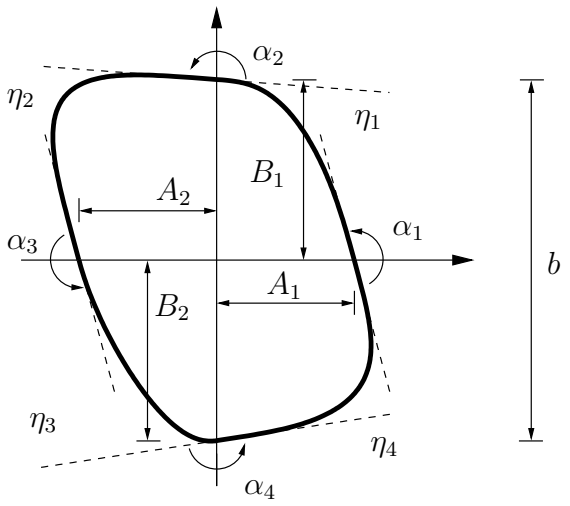

Figure 3: Example of key cross section described by 4 distorted super ellipse, $b = 28\text{mm}$, $A_1 = A_2 = 8\text{mm}$, $B_1 = B_2 = 14\text{mm}$, $\alpha_1 = \alpha_3 = \alpha_4 = 0.2$, $\alpha_2 = -0.1$, and the power $\eta_1 = 3$, $\eta_2 = 4$, $\eta_3 = 2$ and $\eta_4 = 3.5$.

3 Numerical modelling of torsion 2D and 3D

Modelling pure torsion in 2D can be achieved, if we neglect contact modelling, using the warping function Ψ introduced by Saint-Venant, also described in e.g. [6]. Assuming a Cartesian coordinate system with the z-axis aligned with the axial direction the displacements are

$$v_x = -yz\frac{\phi}{l}, \qquad v_y = xz\frac{\phi}{l}, \qquad v_z = \Psi(x,y)\frac{\phi}{l} \tag{9}$$

resulting from the torsional moment

$$T = GJ\frac{\phi}{l} \tag{10}$$

where G is shear modulus of elasticity, J is the cross sectional torsional stiffness factor, ϕ cross sectional angular rotation and l the shaft length. The cross sectional stress components are then

$$\tau_{xz} = \tau_{zx} = (\frac{\Psi}{dx} - y)G\frac{\phi}{l}. \qquad \tau_{xy} = \tau_{yx} = (\frac{\Psi}{dy} + x)G\frac{\phi}{l} \tag{11}$$

The force equilibrium results in the Laplace differential equation assuming no volume force

$$\Delta\Psi = 0 \tag{12}$$

With the correct boundary conditions we can solve this equation numerical to find the displacement v_z, and the shear stress on the cross section. The stress is evaluated by the theoretical shear stress concentration factor

$$K_{ts} = \frac{\tau_{max}}{\tau_{nom}} \tag{13}$$

where maximum shear stress τ_{max} and nominal shear stress τ_{nom} are given by

$$\tau_{max} = (\sqrt{\tau_{zx}^2 + \tau_{zy}^2})_{max} \tag{14}$$

$$\tau_{nom} = \frac{16T}{\pi d^3} \tag{15}$$

In Figure 4 the stress in a shaft, with diameter $d = 100\text{mm}$ and using a keyway as specified in DIN 6885, is shown. The stress concentration is $K_{ts} = 2.93$ when using the maximum fillet as specified by the standard.

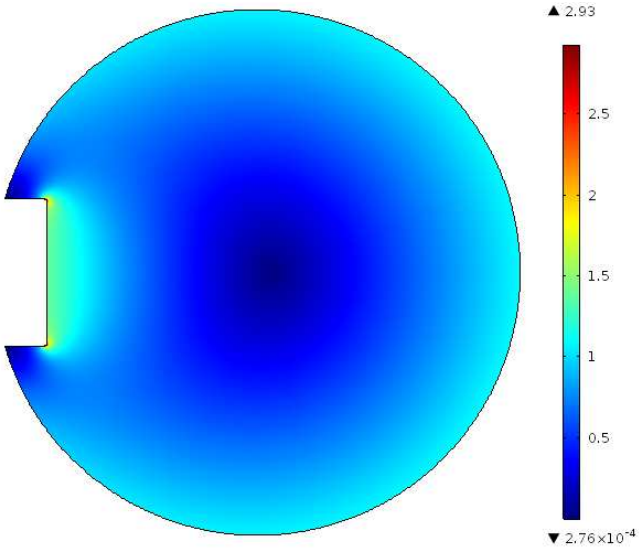

Figure 4: Shear stress ($\sqrt{\tau_{zx}^2 + \tau_{zy}^2}$) in shaft scaled by the nominal stress. The keyway design is according to DIN 6885 for a $d = 100\text{mm}$ shaft with the maximum fillet radius of $r = 0.6\text{mm}$.

For a hub or tube with an internal keyway corresponding to the design in Figure 4 and shown in Figure 5 the maximum stress in the fillet depends on the hub outer diameter. Selecting the stress at the internal diameter of the tube without the keyway as the nominal stress, the stress concentration for the hub is $K_{ts} \approx 3.9$ for outer diameter 3 times greater than internal diameter, as seen in Figure 5. The real stress level is however smaller than in the shaft for transmission of the same torsional moment size due to the larger cross sectional torsional stiffness factor.

Compared to the 2D modelling of pure torsion a full 3D modelling that includes contact modelling is much more involved. The number of elements needed in the Finite Element (FE) mesh is increased considerably for a reasonable stress level convergence. In Figure 6 the stress is shown as a stress concentration factor defined as

$$K_{vM} = \frac{\sigma_{max}^{vM}}{\sigma_{nom}^{vM}} \tag{16}$$

where σ_{max}^{vM} is the maximum von Mises stress and the nominal von Mises stress is defined as

$$\sigma_{nom}^{vM} = \sqrt{3}\frac{16T}{\pi d^3} \tag{17}$$

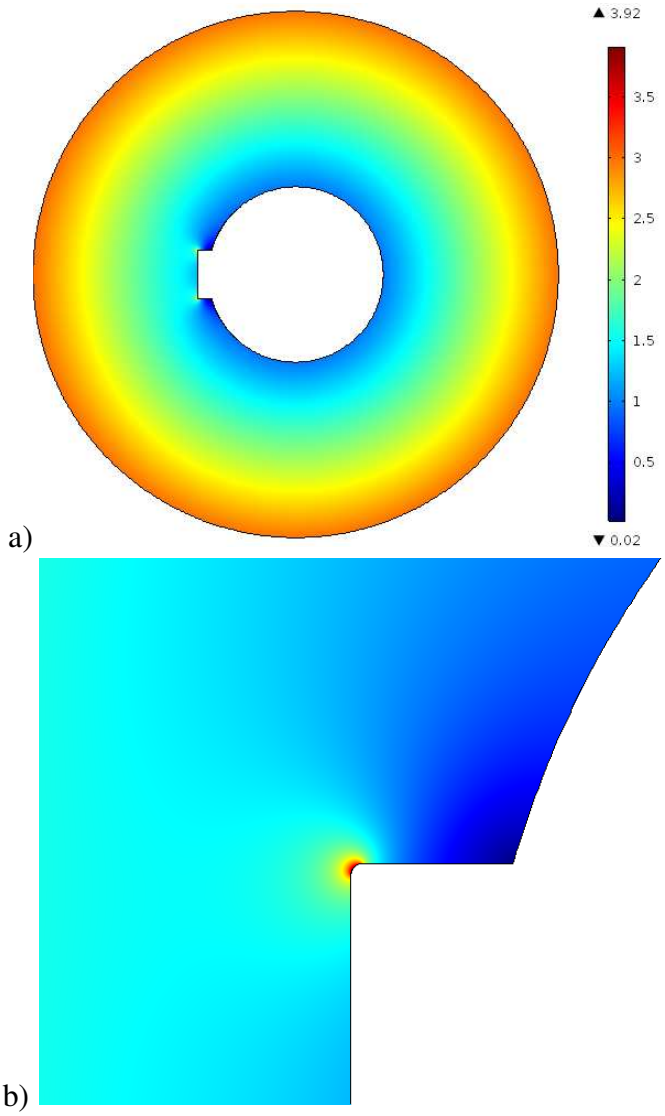

Figure 5: Shear stress ($\sqrt{\tau_{zx}^2 + \tau_{zy}^2}$) in hub scaled by the nominal stress defined as the shear stress on the internal boundary if there were no keyway. The keyway design is according to DIN 6885 for an internal diameter $d = 100\mathrm{mm}$ outer diameter is $d_o = 300\mathrm{mm}$. a) Full design. b) Zoom of fillet.

The applied boundary conditions for the FE model is a symmetry condition on the hub and shaft center plan (in the axial direction), further the hub is clamped on the outer surface. The load/deformation is applied by fixing the outer end of the hub and forcing an axial rotation that leads to a total torsional moment of $T = 200\mathrm{Nm}$ on the hub (i.e. $100\mathrm{Nm}$ on the half model shown). In Figure 6 we have used the minimum key length, $80\mathrm{mm}$, as specified by DIN 6885. We see that in this case we find a stress concentration that is much higher than the one found for the 2D case of pure (individual) shaft and hub torsion, here a value of $K_{vM} = 22.3$ is found. The contact modelling includes a static Coulomb friction, here we use a friction coefficient of $\mu = 0.1$. The contact is modelled using the penalty method and the computations are done in COMSOL [16].

In the FE models we use for 3D models tetrahedral elements and for 2D models triangular elements, in both cases with a quadratic displacement assumption. The stress convergence for the model in Figure 6 is shown in Figure 7, the stress is shown as a function of N (the number of degrees of freedom in the FE model). The mesh with $N = 2.7 \cdot 10^5$ is shown in Figure 8a) and

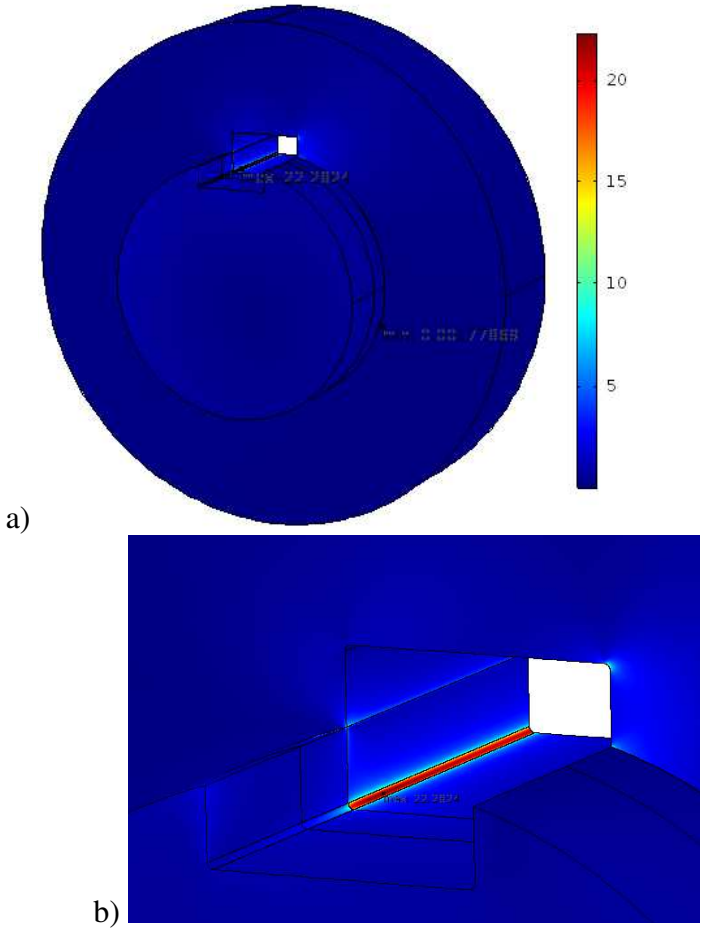

Figure 6: Von Mises stress in hub and shaft (key is hidden) scaled by the nominal stress. The keyway design is according to DIN 6885 for an internal diameter $d = 100\text{mm}$ outer diameter is $d_o = 200\text{mm}$ and length of key is 80mm. a) Full FE design. b) Zoom of fillet.

the mesh with $N = 20.4 \cdot 10^6$ is shown in Figure 8b) and c). The change in the maximum stress when the discretization is increased from $N = 4.4 \cdot 10^6$ to $N = 20.4 \cdot 10^6$ is approx. 1% i.e. we consider the stress to be converged for the last model with the stress level being $K_{vM} = 22.3$.

As seen the model must be highly refined. The highest stress is found in the shaft in the fillet in the keyway bottom. The stress along the keyway in the center plan is shown in Figure 9. The stress is shown from the contacting side towards the side without contact, i.e. both the sides and the bottom of the keyway is shown. It is clear due to the stress peak that there is a large potential for reducing the maximum stress.

For optimization the full size FE model as presented is not feasible to use due to the large number of degrees of freedom and the associated computational time. However it is clear that the modelling must include contact modelling.

One possibility for reducing the computer time is to reduce the number of elements. One way to do this is to reduce the hub width, in Figure 10 the stress along the keyway in the center plan is shown for different hub width, the minimum element size is kept fixed. In the analysis the rotation angle is kept fixed meaning that the transferred torsional moment is reduced with reduced hub width. In Figure 10 the stress is scaled for all cases such that the maximum stress is unity. We see that that for the contacting part (approximately the first quarter of the arc length) the variation in shape is limited if the width is reduced to $W = 20\text{mm}$, and for all cases the peak stress shape is identical. This indicated that an optimization could be performed on the

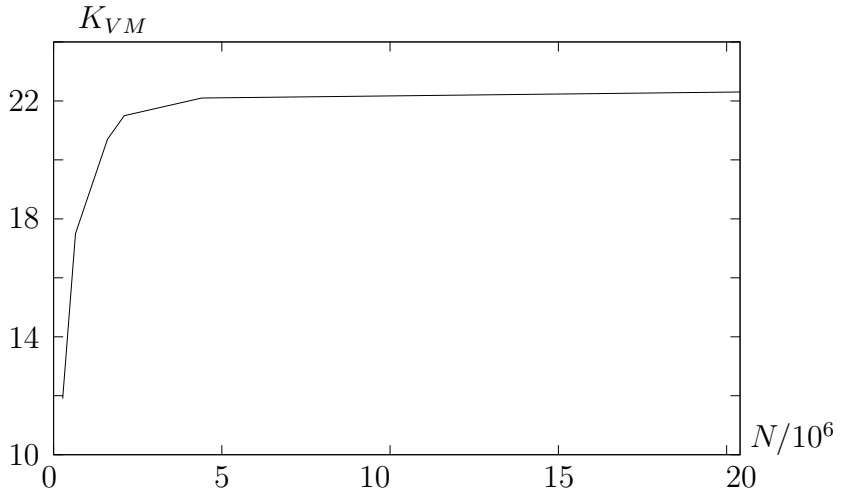

Figure 7: Maximum Von Mises stress scaled by the nominal stress as a function of degree of freedom in the FE model. For the keyway design seen in Figure 6.

model with the reduced hub width.

One further possibility for reducing the computational time is to increase the element size. It is still important that the stress variation is described sufficiently accurate. In Figure 11 the stress variation for a reduced model is compared to the highly refined model. The computational time is reduced here with a factor of 50. The reduced model cannot estimate the maximum stress with sufficient accuracy, however the reduced model describes the stress variation sufficiently accurate for the optimization purpose.

A 2D model including contact is also possible. For a 2D model the problem is how the boundary conditions should be applied. For the result in Figure 12 we have fixed the hub outer rim and a forced rotation is applied to the shaft at a minor circle with a diameter $d/10$. The rotation size is made such that the transferred torsional moment is $T = 200\mathrm{Nm}$. In the modelling an assumption of plain strain is applied. Due to the model being 2D we can increase the number of elements along the contacting boundaries.

In comparing the results from the two models we see that that the overall stress distribution is reasonably described by the 2D model when comparing with the full model. It is noted that the stress peak for the 2D model is smaller in value and also there is a variation in the stress over the circular fillet arc in the keyway corner.

For the optimization in the next sections the 2D contact model is used. All examples are with a shaft diameter of $100\mathrm{mm}$ and the transferred torsional moment is $200\mathrm{Nm}$. The final result is then verified by the full 3D modelling. In all the modelling we assume a prefect initial fit between the three parts. The reason being that this makes a direct comparison between the different designs possible. This point was also discussed in [13].

4 Optimized symmetric key design

In [6] different optimized designs were shown. The optimization was performed without the key and contact modelling, i.e. it was modelled as pure torsion using the Saint-Venant warping function. Three different keyway/key designs were presented depending on the level of allowable design changes. The designs are all symmetric, and the only change relative to the standard is that the circular arc is substituted by a super ellipse, as seen in the key quarter model in Figure

a)

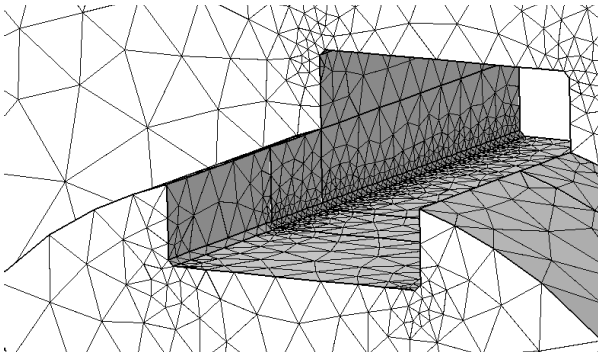

b)

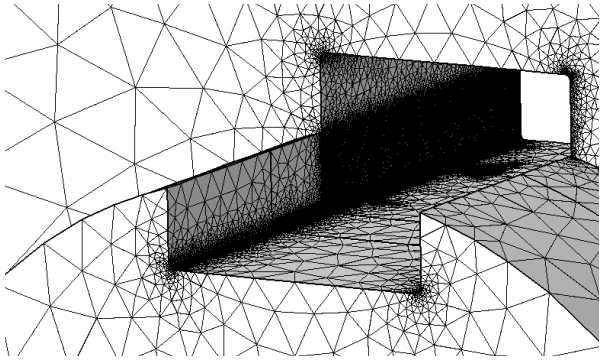

c)

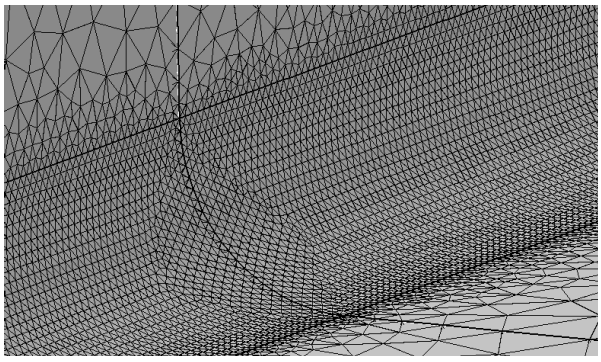

Figure 8: Illustration of mesh for FE model in Figure 6 (key is hidden). a) Mesh with $N = 2.7 \cdot 10^5$ b) Mesh with $N = 20.4 \cdot 10^6$. c) Zoom of fillet for mesh with $N = 20.4 \cdot 10^6$.

13.

The three optimized results are repeated here but now with the 2D contact modelling for comparison. The design variables (constraint/unconstraint) for the three designs are

- Design I, Constraint variables: $b = 28\text{mm}$, $h = 16\text{mm}$, $L_1 = 7.4\text{mm}$. Design variables $L_2 = 13.19\text{mm}$, $\eta = 1.63$
- Design II, Constraint variables: $b = 28\text{mm}$, $L_1 = 7.4\text{mm}$. Design variables $h = 23.02\text{mm}$, $L_2 = 0\text{mm}$, $\eta = 1.99$
- Design III, $b = 28\text{mm}$, $h = 16\text{mm}$. Design variables $L_1 = 4.56\text{mm}$, $L_1 = 0\text{mm}$, $\eta = 2.22$

For Design I the constraint values are in accordance with the DIN 6885-1 standard. In Design II a larger key is allowed while Design III as Design I fits within the standard key area. The result from the 2D contact simulation is shown in Figure 14.

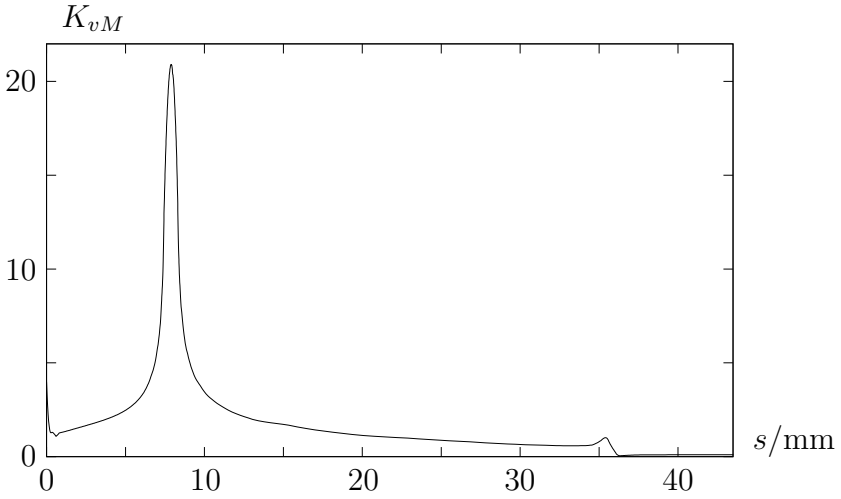

Figure 9: Stress along shaft keyway at the center plan. The stress is shown as von Mises stress scaled by the nominal stress.

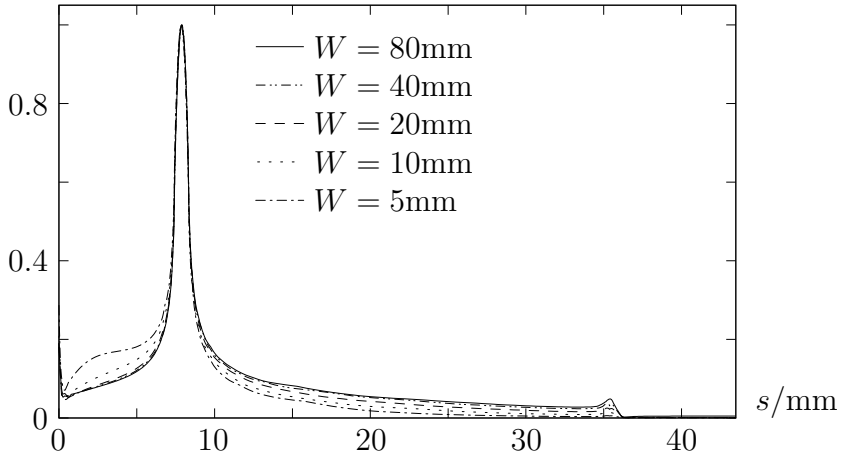

Figure 10: Illustration of stress distribution along shaft keyway at the center plan depending on the hub width. The stress for the different length are all scaled so that the maximum stress is unity.

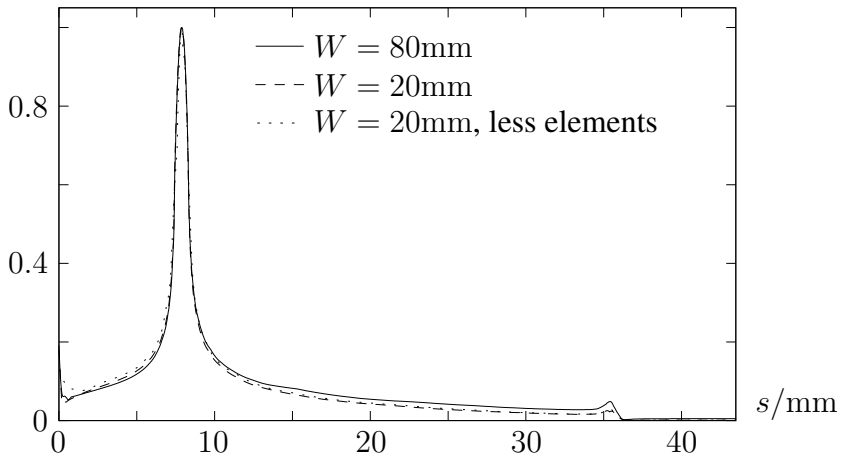

Figure 11: Illustration of stress distribution along shaft keyway at the center plan. The stress for the different models are all scaled so that the maximum stress is unity.

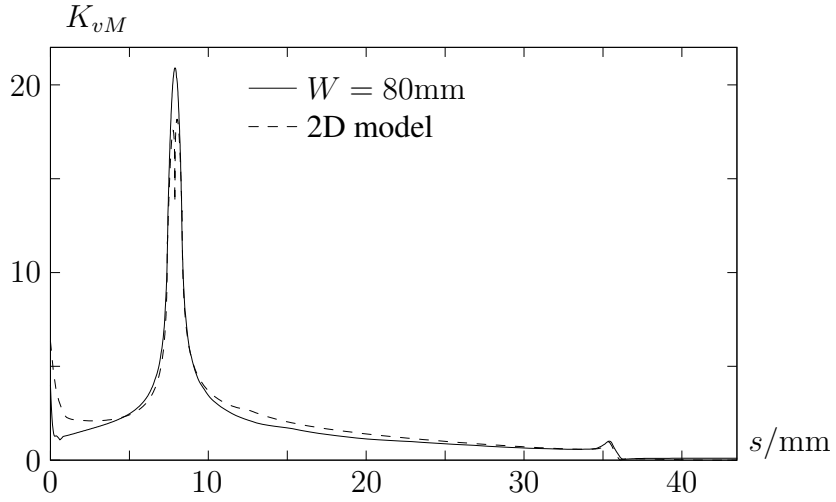

Figure 12: Stress along shaft keyway at the center plan for the full 3D model and for the 2D model. The stress is shown as von Mises stress scaled by the nominal stress.

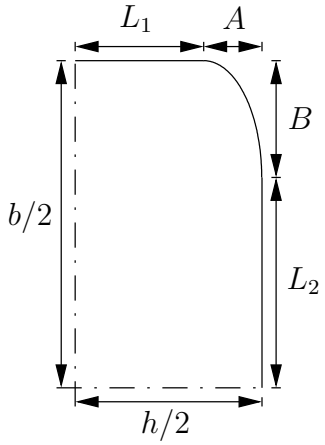

Figure 13: Key/keyway quarter design.

The stress concentrations are in all cases not identical to the reported results from pure torsion. The relative design improvements when compared to the DIN standard is however still significant for Designs II and III. Design II has the largest improvement with a stress reduction of 63% while design III has a reduction of 41%.

The cross sectional key area is important for the possible improvement in the stress level, with a larger area a larger reduction in the maximum stress can be found. This can also be observed in comparing Design II and III. In the remaining part of the paper the key cross sectional area is constrained to be smaller than the original DIN design.

Performing the parametric optimization instead, directly using the 2D contact model and the design variable as presented in Figure 3 we obtain significant reductions in the stress concentration. We first enforce double symmetry i.e. the only design variable is η_1. The optimized result is $\eta_1 = 3.1$ and stress distribution is shown in Figure 15.

The stress concentration is here $K_{vM} = 5.9$ which is a reduction of 67% compared to the DIN design. We notice that the maximum stress is now found in both the shaft and hub.

We also have the possibility for a single symmetric design with the two design variables $\eta_1 = \eta_4$ and $\eta_2 = \eta_3$ (see Figure 3). The optimization result is $\eta_1 = 2.4$ and $\eta_2 = 5.6$, the stress distribution is shown in Figure 16.

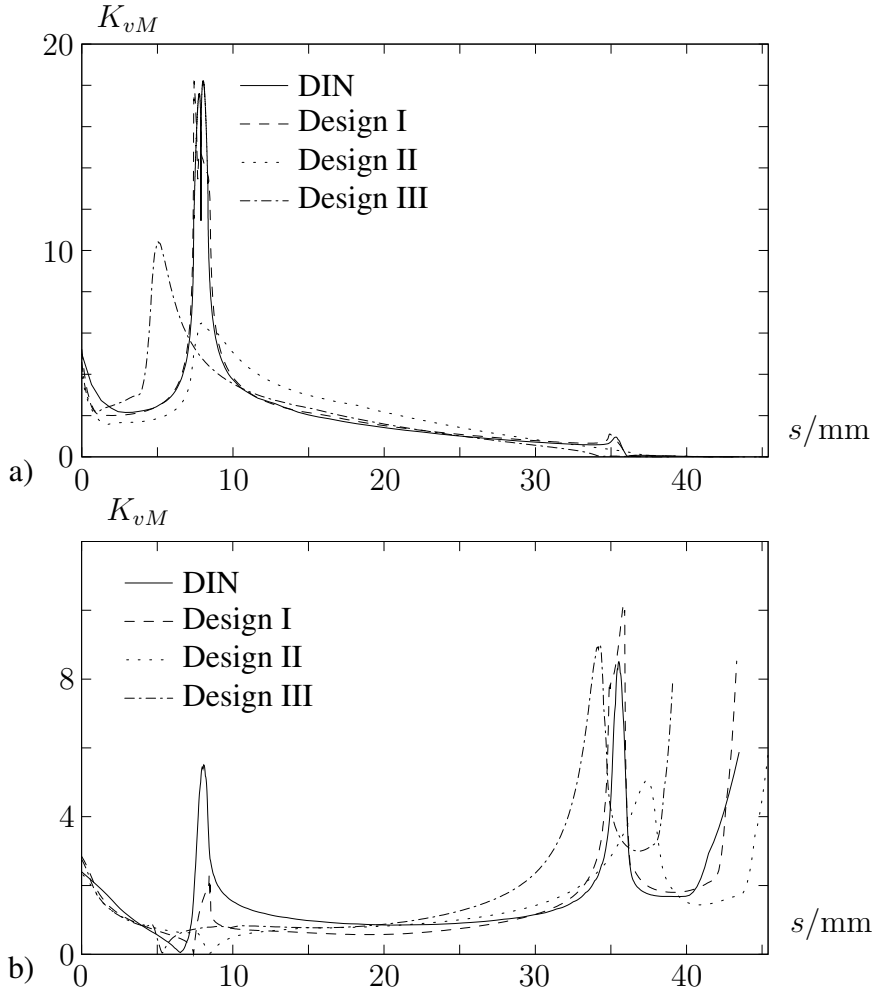

Figure 14: Stress along the keyway. The stress is shown as von Mises stress scaled by the nominal stress. a) Stress in shaft keyway for the four designs. b) stress in hub keyway for the four designs.

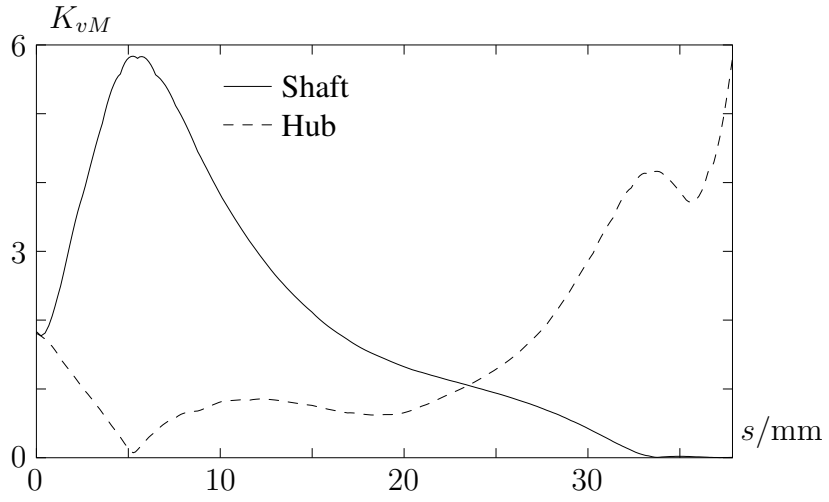

Figure 15: Optimized double symmetric design. Stress along shaft and hub keyway. The stress is shown as von Mises stress scaled by the nominal stress.

With this design we have a further reduction in the stress level, $K_{vM} = 5.0$, which is a

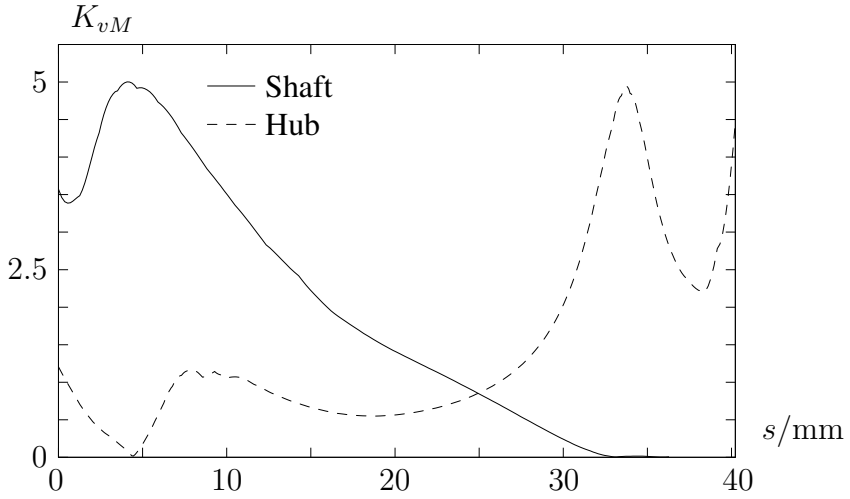

Figure 16: Optimized single symmetric design. Stress along shaft and hub keyway. The stress is shown as von Mises stress scaled by the nominal stress.

reduction of 72% compared to the DIN design.

With the two symmetric designs the torsional moment can still be applied in both direction equally well. If we allow for unsymmetrical designs the stress can be reduced even further.

5 Optimized unsymmetrical key design

If the torsional moment in the shaft hub connection is only applied in one direction we can make an unsymmetrical design. The key shape is in the present paper controlled by the design parameterization shown in Figure 3. This parameterization has 13 design parameters. In order for the design to be feasible for production but also for application we constrain two of the angles $\alpha_2 \geq 0$ and $\alpha_4 \geq 0$. From numerical experiments it is clear that the important boundary to design is where the contact is applied to both the shaft and hub. Assuming that the torsional moment is applied in clockwise direction (on the shaft) it is the design of the key in the quadrant 2 and 4 that is important (see Figure 3). For this reason the following values are selected/constraint

$$b = 28\mathrm{mm}, \qquad B_1 = B_2 = 26\mathrm{mm} \qquad \eta_1 = \eta_3 = 2$$

In the two quadrants where we do not have contact the design of the keyway is simplified to a straight line instead of the super ellipse. The straight lines are extended to the surface of the hub and shaft respectively. This leaves 8 design parameters for the optimization.

With the further reduction in the stress level the stress increases at the run-out of contact between the key and hub becomes significant. The reason is that the corner is too stiff, the same point was addressed in [8]. One possibility to overcome this problem is to reduce the stiffness by removing material. The shape and size of this stiffness relief/material removal is not highly important as long as this does not give rise to a higher stress than the one found in the contact between key, hub and shaft. The simple design shown in Figure 17 is selected.

Using this design for the stiffness relief and the selected 8 design parameters the optimized solution is

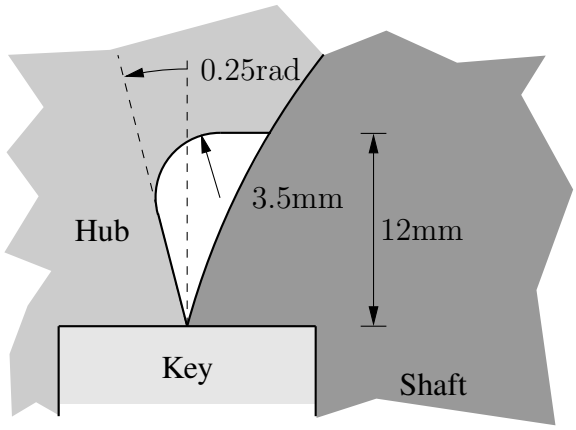

Figure 17: Design of stiffness relief.

$$\alpha_1 = 0.57\text{rad}, \qquad \alpha_2 = 0,$$
$$\alpha_3 = 0.57\text{rad}, \qquad \alpha_4 = 0.26\text{rad}$$
$$\eta_2 = 2, \qquad \eta_4 = 2.2,$$
$$A_1 = (1 + 5\tan(\alpha_1))\text{mm}, \qquad A_2 = (1 + 2\tan(\alpha_3))\text{mm}$$

The unsymmetrical key and keyway design and the stress level is shown in Figure 18.

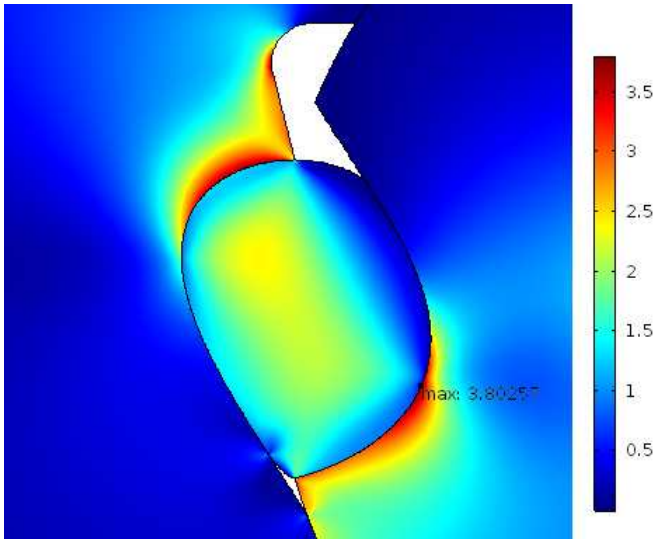

Figure 18: Design of optimized unsymmetrical key. The scale indicated von Mises stress scaled by the nominal stress.

The stress along the keyway in the shaft and hub together with the stress along the stiffness relief is shown in Figure 19

As shown in Figure 19 the design is made such that we have almost equal maximum stress at both hub and shaft. We also see that the stress is constant over a larger part of the contact length. The maximum stress in the relief grove is kept at approximately the same level. The maximum stress concentration is for the shown design $K_{vM} = 3.80$ which is a reduction of 78% compared to the DIN design. The stress variation indicates that a further reduction in the

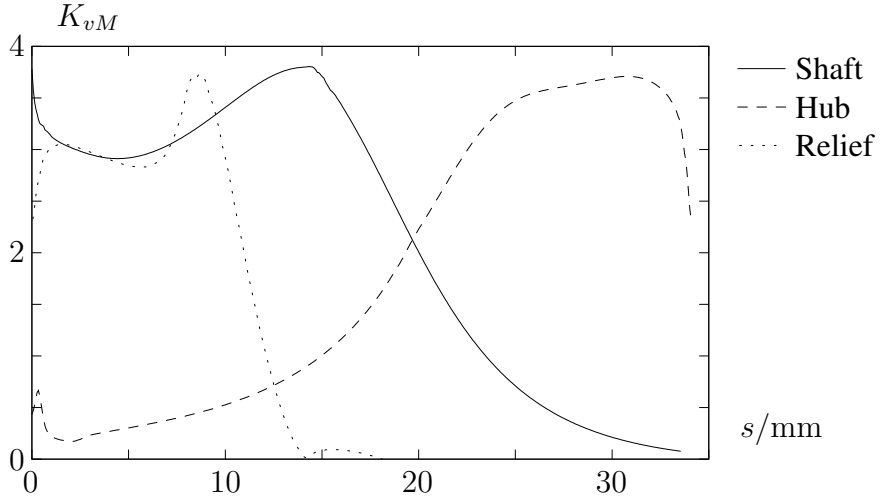

Figure 19: Optimized unsymmetrical design. Stress along shaft and hub keyway and also along the stiffness relief. The stress is shown as von Mises stress scaled by the nominal stress.

stress level might be possible with a more involved parameterization. The design is not highly sensitive to variation in the design variables and when comparing to the best symmetric design it can be discussed if this further reduction in stress level is needed.

For verification the optimized design is used in a 3D simulation of the same design. It is clear that the result as shown in Figure 20 and Figure 21 is not identical to the one found in the 2D modelling but overall the results are confirmed. In the 3D simulation there is also the run-out of contact in the axial direction that leads to an increased stress level. Here the maximum stress concentration found is $K_{vM} = 7.08$, whereas in the center plane the value is $K_{vM} = 4.88$. The reduction of the stress level due to the run-out in axial direction is not investigated further in the present paper.

The stress level found in the center plane still corresponds to a stress reduction of 78%, which confirms the findings from 2D and illustrates that it is possible to use the 2D model. Doing the optimization directly on the 3D model is infeasible, the shown model has $14 \cdot 10^6$ degrees of freedom, with a computational time on a regular PC of $8\mathrm{h}$.

The stress level is throughout the paper found using numerical FE calculation, no experimental verification is made. However the same level of mesh refinement is used for the different designs so the relative change in stress level for the optimized design when compared to the standard design is considered to be valid.

6 Conclusion

In the present paper we use shape optimization to improve the strength of key connections between shaft and hub. The numerical modelling of applying torsional moment is investigated. The necessary modelling refinement is important for the subsequent optimization procedure. Including contact modelling is shown to be necessary for the fatigue strength evaluation. A full 3D contact modelling is possible but a 2D contact modelling, with a much higher computational efficiency, is sufficient for design optimization.

Previous designs optimized using an assumption of pure torsion is re-evaluated using contact modelling. The evaluation shows that the proposed designs still exhibits a large improvement in the maximum stress level relative to the standard DIN design.

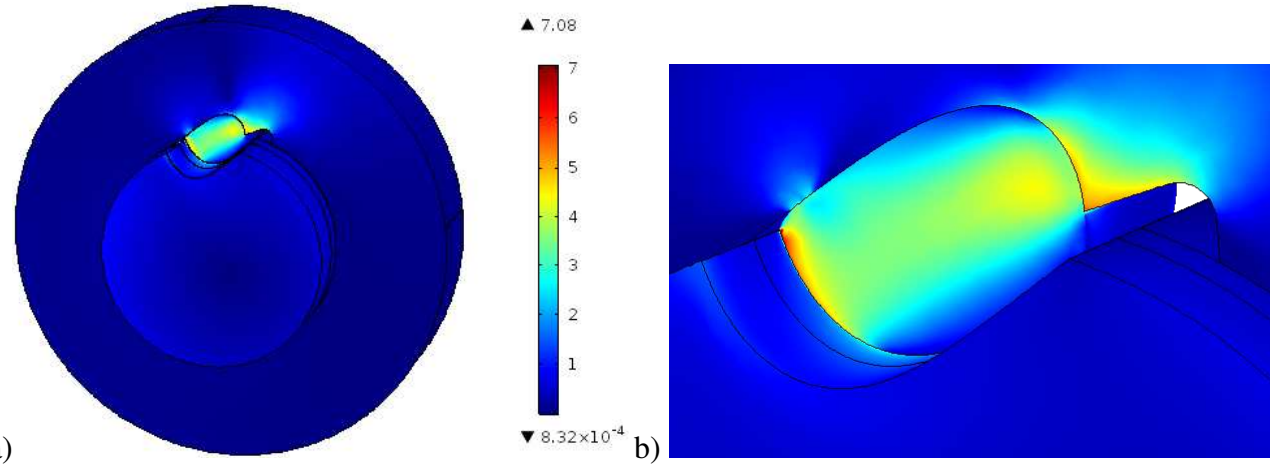

Figure 20: 3D model of optimized non-symmetrical key. The Von Mises stress is scaled by the nominal stress. a) Full FE design. b) Zoom of key.

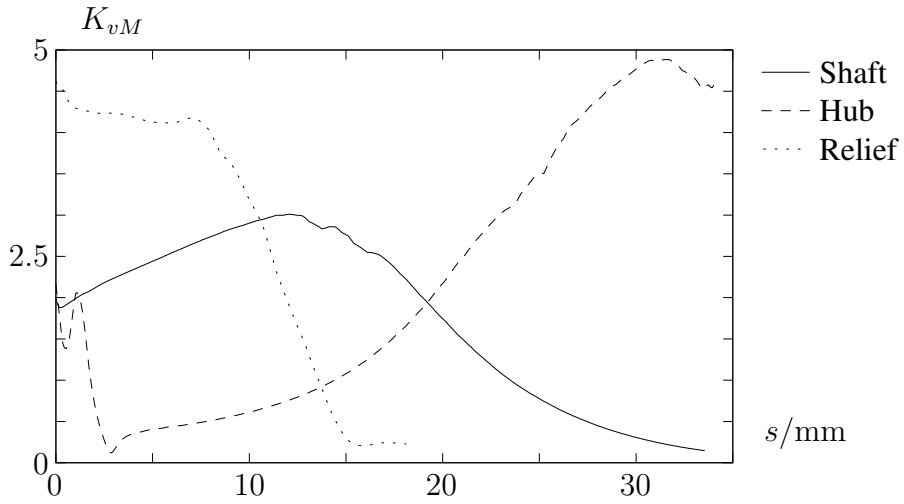

Figure 21: 3D results for optimized unsymmetrical design. Stress along shaft and hub keyway and also along the stiffness relief at the center plan. The stress is shown as von Mises stress scaled by the nominal stress.

Parameterization of the key shape can be performed in many ways, in the present paper a design parameterization based on the super ellipse is presented. Using the proposed parameterization and the 2D contact modelling it is found that the maximum stress level can be reduced even further as compared to the previous proposed designs. The new key design is constrained to have a cross sectional area not greater than the original DIN design, the reason for this is to make a direct comparison possible. If the area is not fixed, even larger stress reductions can be achieved. Prescribing the design to be symmetric the maximum stress is reduced by 72%. Allowing for an unsymmetrical design the reduction in maximum stress is 78%.

It can be argued that the improvement achieved by the symmetric design and the associated simplicity might make this the more practical design.

Acknowledgment
For discussions and suggestions I wish to thank Prof. Peder Klit.

References

[1] DIN 6885-1. Paßfedern nuten (in German), 1968.

[2] Norton RL. *Machine design: An integrated Approach*. Pearson, 2020.

[3] Budynas R and Nisbett K. *Shigley's Mechanical Engineering Design*. McGraw Hill, 2020.

[4] Pilkey WD, Pilkey DF and Zhumning B. *Peterson's stress concentration factors, 4th Edition*. John Wiley & Sons, inc., 2020. 640 pages.

[5] Peterson RE. Fatigue of shafts having keyways. *American Society for Testing Materials - Proceedings* 1932; 32(part 2): 413–419.

[6] Pedersen NL. Stress concentrations in keyways and optimization of keyway design. *Journal of Strain Analysis for Engineering Design* 2010; 45(8): 593–604.

[7] Orthwein WC. A new key and keyway design. *J Mech Des Trans ASME* 1979; 101(2): 338–341.

[8] Pedersen NL. On optimization of interference fit assembly. *Structural and Multidisciplinary Optimization* 2016; 54(2): 349–359.

[9] Fessler H, Rogers CC and Stanley P. Stresses at end-milled keyways in plain shafts subjected to tension, bending, and torsion. *Journal of Strain Analysis* 1969; 4(3): 180–189.

[10] Okubo H, Hosono K and Sakaki K. The stress concentration in keyways when torque is transmitted through keys. *Experimental Mechanics* 1968; 8(8): 375–380.

[11] Ding Y. Shape optimization of structures: A literature survey. *Computers and Structures* 1986; 24(6): 985–1004.

[12] Pedersen NL. Stress concentration and optimal design of pinned connections. *Journal of Strain Analysis for Engineering Design* 2019; 54(2): 95–104. DOI: 10.1177/0309324719842766.

[13] Pedersen NL. On optimal stress for shaft-hub connections (polygon connections). *Journal of Strain Analysis for Engineering Design* 2021; 56(4): 195–205. DOI: 10.1177/0309324720969530.

[14] Pedersen NL. Improving bending stress in spur gears using asymmetric gears and shape optimization. *Mechanism and Machine Theory* 2010; 45(11): 1707–1720.

[15] Pedersen NL. Minimizing tooth bending stress in spur gears with simplified shapes of fillet and tool shape determination. *Engineering optimization* 2015; 47(6): 805–824.

[16] COMSOL AB. www.comsol.com: Stockholm, Sweden, 1986 -.

Appendix

Notation

b	Width of key (Design variable)
d	Diameter of shaft
h	Height of key (Design variable)
l	Lenght of shaft
v_x	Displacement in x direction
v_y	Displacement in y direction
v_z	Displacement in z direction
A	Super elliptic principle axes (Design variable)
A_1	Super elliptic principle axes (Design variable)
A_2	Super elliptic principle axes (Design variable)
B	Super elliptic principle axes (Design variable)
B_1	Super elliptic principle axes (Design variable)
B_2	Super elliptic principle axes (Design variable)
G	Shear modulus
J	Cross sectional torsional stiffness factor
K_{ts}	Theoretical shear concentration factor
K_{vM}	Theoretical von Mises stress concentration factor
L_1	Length (design parameter)
L_2	Length (design parameter)
T	Torsional moment
W	Width of hub
α_1	Angle (Design variable)
α_2	Angle (Design variable)
α_3	Angle (Design variable)
α_4	Angle (Design variable)
β	Angle
η	Super elliptic power (Design variable)
η_1	Super elliptic power (Design variable)
η_2	Super elliptic power (Design variable)
η_3	Super elliptic power (Design variable)
η_4	Super elliptic power (Design variable)
γ	Angle
ϕ	Cross sectional angular rotation
μ	Coefficient of static friction
σ	Normal stress
τ	Shear stress
Ψ	Warping function